THE JOURNAL OF BIOLOGICAL CHEMISTRY
Vol. 275, No. 24, Issue of June 16, pp. 18271–18278, 2000

Printed in U.S.A.

HIV-1 Reverse Transcriptase-Pseudoknot RNA Aptamer Interaction Has a Binding Affinity in the Low Picomolar Range Coupled with High Specificity*

Received for publication, February 16, 2000, and in revised form, March 29, 2000
Published, JBC Papers in Press, April 4, 2000, DOI 10.1074/jbc.M001309200

Oliver Kensch‡, Bernard A. Connolly§¶, Heinz-Jürgen Steinhoff‡, Alistair McGregor§, Roger S. Goody‡, and Tobias Restle‡‖

From the ‡Max-Planck-Institut für molekulare Physiologie, Abteilung Physikalische Biochemie, Otto-Hahn-Straße 11, 44227 Dortmund, Germany and the §School of Biochemistry and Genetics, University of Newcastle, Newcastle upon Tyne, NE2 4HH, United Kingdom

Systematic evolution of ligands by exponential enrichment (SELEX) is a powerful method for the identification of small oligonucleotides that bind with high affinity and specificity to target proteins. Such DNAs/RNAs are a new class of potential chemotherapeutics that could block the enzymatic activity of pathologically relevant proteins. We have conducted a detailed biochemical study of the interaction of human immunodeficiency virus 1 (HIV-1) reverse transcriptase (RT) with a SELEX-derived pseudoknot RNA aptamer. Electron paramagnetic resonance spectroscopy of site-directed spin-labeled RT mutants revealed that this aptamer was selected for binding to the "closed" conformation of the enzyme. Kinetic analysis showed that the RNA inhibitor bound to HIV RT in a two-step process, with association rates similar to those described for model DNA/DNA and DNA/RNA substrates. However, the dissociation of the pseudoknot RNA from RT was dramatically slower than observed for model substrates. Equilibrium binding studies revealed an extraordinarily low K_d, of about 25 pM, for the enzyme-aptamer interaction, presumably a consequence of the slow off-rates. Additionally, this pseudoknot aptamer is highly specific for HIV-1 RT, with the closely related HIV-2 enzyme showing a binding affinity close to 4 orders of magnitude lower.

HIV[1] reverse transcriptase (RT), a key enzyme of the retroviral life cycle, catalyzes the conversion of the single stranded genomic viral RNA into double stranded proviral DNA, which in turn is integrated into the host genome. The enzyme consists of an asymmetric heterodimer of two subunits, p66 and p51, possessing RNA- and DNA-dependent DNA polymerase and RNase H activities. The small subunit, p51, is derived from p66 by proteolytic cleavage of the C-terminal domain. Several x-ray structures of RT have been determined showing structural changes of the enzyme depending on whether the protein is bound to inhibitors, bound to substrates, or unliganded (for a recent review, see Ref. 1). The overall fold of the p66 subunit has been compared with a right hand, consisting of subdomains termed fingers, palm, thumb, connection, and RNase H.

RT is one of the main targets in the fight against AIDS. Drugs currently in use include nucleoside inhibitors, such as AZT, 3TC, ddI, ddC, d4T, as well as non-nucleoside inhibitors, such as nevirapine, delavirdine, and efavirenz, all of which target RT (for a review, see Ref. 2). However, severe side effects and the rapid emergence of drug resistant mutants compromise the efficacy of these drugs. Recently, significant progress has been achieved by applying multidrug combination therapy (for a review, see Ref. 3). In this therapy, at least two drugs against RT and one against the retroviral protease are taken simultaneously. Nevertheless, the underlying problems of this kind of chemotherapeutic treatment remain the same, urgently calling for alternative strategies to deal with viral infections such as AIDS.

Many different strategies have been discussed without, so far, leading to a genuine alternative to the currently used anti-AIDS drugs. However, one promising alternative approach could be the application of nucleic acid aptamers derived using *in vitro* selection. Aptamers bind with high affinity as well as specificity to their target proteins, often eliminating enzymatic activity (for a review, see Ref. 4). Tuerk and Gold (5) have used SELEX to identify RNA aptamers against the HIV-1 RT. The analysis of the isolated aptamers revealed a consensus sequence that resulted in the formation of an RNA pseudoknot (6). The interactions between SELEX RNA pseudoknots and HIV-1 RT have been analyzed in some detail using biochemical studies and chemical modification (7, 8).

Pseudoknots are defined as loop regions base pairing with complementary sequences, outside the loop, in the same RNA molecule (9, 10). The pseudoknot fold is a widespread structural motif found in all kinds of RNA, including coding and noncoding regions of cellular mRNAs, viral RNAs, ribosomal RNAs, and small nuclear RNAs. Although not all of the functions of this RNA secondary structure motif are fully understood, pseudoknots play an important role in ribosomal frameshifting, in transcriptional read-through, as internal ribosomal entry sites, and as translational enhancers, and they are key components of ribozymes (11) and cis-acting elements important for the initiation of viral replication (for a review, see Ref. 12). Several NMR studies and one high resolution x-ray study of pseudoknots have been reported (13–19).

The x-ray structure of HIV-1 RT complexed with an RNA

* The costs of publication of this article were defrayed in part by the payment of page charges. This article must therefore be hereby marked "*advertisement*" in accordance with 18 U.S.C. Section 1734 solely to indicate this fact.

¶ Supported by a United Kingdom Medical Research Council Senior Research Leave fellowship. Part of this work was carried out while this author was on sabbatical in Dortmund. A CIBA Fellowship Trust award contributed toward the cost of this sabbatical.

‖ To whom correspondence should be addressed. Tel.: 49-231-133-2364; Fax: 49-231-133-2398; E-mail: tobias.restle@mpi-dortmund.mpg.de.

[1] The abbreviations used are: HIV, human immunodeficiency virus; EIAV, equine infectious anemia virus; RT, reverse transcriptase; SELEX, systematic evolution of ligands by exponential enrichment; EPR, electron paramagnetic resonance; p/t, primer/template; HEX, hexachlorofluorescein; DTT, dithiothreitol.

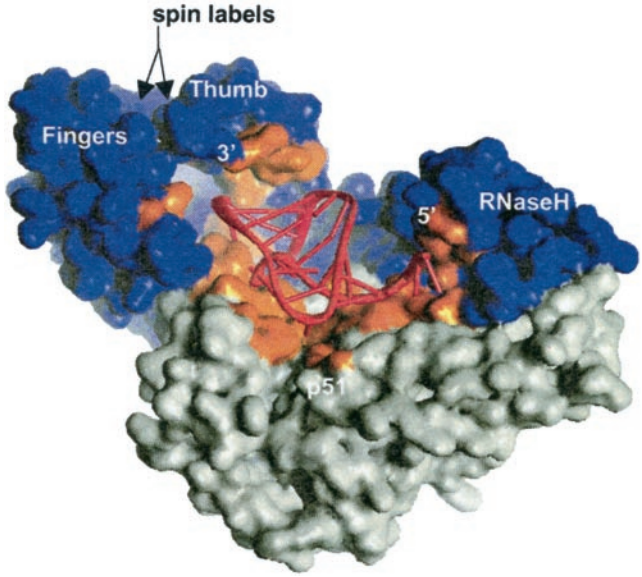

FIG. 1. **Structure of the HIV-1 RT pseudoknot RNA complex.** The p66 subunit is shown in *blue,* the p51 subunit in *gray,* and the RNA in *red*. Surface residues <5 Å away form the RNA aptamer are shown in *orange*. The positions of the two spin labels used for the EPR measurements at the tip of the fingers and thumb domain of the p66 subunit are indicated.

pseudoknot inhibitor has been solved recently (see Fig. 1) (20). This is the first example of an x-ray structure of such an pseudoknot aptamer bound to its target protein. The RNA ligand binding surface lies within the nucleic acid cleft of the enzyme, between the polymerase and RNaseH active sites, and partially overlapping the binding surface of duplex DNA substrates. The pseudoknot is kinked by 60° from the co-axial stacking of stems 1 and 2, thus optimizing the extensive contacts between the RNA inhibitor and both subunits of the heterodimeric enzyme. The protein-RNA interaction stabilizes the "closed" conformation of the enzyme, in which the fingers and thumb domains of the large subunit are in close contact. Further, we suggested that the SELEX procedure appears to have identified an RNA molecule whose uncomplexed solution structure is very similar to its structure when bound to RT and which binds to the unliganded conformation of RT.

Here we present the first detailed biochemical study of the this enzyme-inhibitor interaction. Using electron paramagnetic resonance (EPR) spectroscopy of site-directed spin-labeled RT mutants, we show that the relative positions of the fingers and thumb domains of the large subunit are virtually indistinguishable whether or not RNA is bound. This proves, for the first time, that RT in solution can adopt the closed conformation seen in the x-ray structure by Rodgers *et al.* (21) and might be an important feature of selecting for tight binding ligands. An analysis of the binding equilibrium of the protein-inhibitor complex revealed astonishingly tight binding, with a K_d in the low picomolar range, about 2–3 orders of magnitude lower than the K_d of about 5 nM reported earlier by Tuerk *et al.* (6). To our knowledge, this is the first report of a SELEX-derived RNA ligand showing such a tight binding for a known nucleic acid binding target protein.

EXPERIMENTAL PROCEDURES

Mutagenesis of Reverse Transcriptase—To label RT with either spin labels or fluorophors in a site-directed manner, the naturally occurring cysteines had to be replaced by serines, and cysteines had to be introduced at the desired positions. In a first step, the mutant RT $p66^{C38S/C280S}/p51^{C280S}$ was generated. The cysteine at position 38 in the small subunit is not solvent-accessible and consequently does not interfere with site-directed labeling.[2] In a second step, cysteines at certain positions were introduced as described below.

Mutant RT was prepared by site-directed mutagenesis using polymerase chain reaction (22). The mutations were introduced into the plasmids $pRT1_{66}$ (23) and p6HRT51 (24). The plasmids thus generated were transformed into *Escherichia coli* M15/pDMI.1 (25), resulting in expression systems for mutated p66 and mutated His-tagged p51.

Protein Purification—Recombinant heterodimeric wild type HIV-1, HIV-2, and equine infectious anemia virus (EIAV) RT were expressed in *E. coli* and purified as described before (23, 26, 27). Enzyme concentrations were routinely determined using an extinction coefficient at 280 nm of 260,450 (HIV-1 RT), 238,150 (HIV-2 RT), and 223,180 $M^{-1}\ cm^{-1}$ (EIAV RT). The purified RTs were free of nuclease contamination.

Mutant RTs were purified according to a protocol described previously (28). Co-homogenization of *E. coli* cells expressing p66 or p51 led to reconstruction of heterodimeric p66/p51 RT. Analysis of the mutant proteins by a standard RT assay (see below) showed indistinguishable polymerase activity as compared with the wild type enzyme.

Labeling of RT Mutants—Spin labeling of the introduced cysteine residues at positions 24 and 287 in p66 was achieved by the following procedure. In order to reduce any disulfide bonds, 2 μl of 1 M DTT was added to 200 μl of a 44 μM solution of mutant RT ($p66^{W24C/C38S/C280S/K287C}/p51^{C280S}$) in Buffer A. After 30 min at 4 °C, a 2-fold excess of 18/36-mer DNA/DNA p/t was added to the solution. The resulting RT-p/t complex was separated from excess DTT using a Sephadex G25 gel filtration column (Amersham Pharmacia Biotech). The eluted complex was collected in a tube containing 2 μl of 100 μM (1-oxyl-2,2,5,5-tetramethylpyrroline-3-methyl)methane-thiosulfonate (Toronto Research Chemicals, Inc.) in Me_2SO. After 16 h at 4 °C, excess spin label and bound p/t were removed by purifying the enzyme over a Ni^{2+}-nitrilotriacetic acid-Sepharose column (Qiagen). The bound protein was washed extensively with a buffer containing 1 M NaCl and eluted with 0.3 M imidazole. Subsequently, the protein solution was concentrated, and buffer was changed (50 mM Tris-HCl, pH 8.0, 25 mM NaCl, 6 mM $MgCl_2$, 10% glycerol) using centrifugal filters (Millipore). Finally, samples were shock-frozen in liquid nitrogen and stored at −80 °C. The labeled cysteine/RT ratio, estimated from double integration of the EPR spectra and absorption measurements of protein (280 nm), was found to be > 90%. Analysis of the spin-labeled protein by a standard RT assay (see below) shows polymerase activity that was indistinguishable from that of wild type enzyme.

The labeling of the HIV-1 RT mutant ($p66^{C38S/C280S}/p51^{C280S/K281C}$) used for the fluorescence resonance energy transfer experiments at position $p51^{281C}$ with the fluorophor $Alexa_{488}$ was performed according to the instructions given by the manufacturer (Molecular Probes). Equilibrium as well as kinetic measurements of DNA/DNA p/t binding to this fluorescently labeled RT gave similar values to those obtained for the wild type protein (data not shown).

RNA Preparation—The 33-nucleotide pseudoknot RNA (sequence, 5′-GGGAGAUUCCGUUUUCAGUCGGGAAAAACUGAA) was prepared in a standard 10-ml T7 reaction mixture for *in vitro* transcription and purified by gel electrophoresis as described previously (20, 29). The RNA was refolded at a concentration of 200–300 μM at 65 °C for 5 min followed by slow cooling to room temperature in 20 mM cacodylate buffer, pH 6.5, 25 mM NaCl, and 5 mM $MgCl_2$. 5′-End labeling of the RNA with T4 polynucleotide kinase (New England Biolabs) was performed as described previously (30). Dephosphorylation of the *in vitro* transcribed RNA prior to end labeling was carried out according to standard procedures (31). The fluorescent-labeled 5′-hexachlorofluorescein (HEX) pseudoknot RNA was synthesized and high pressure liquid chromatography-purified as described previously (32). HEX phosphoramidite was obtained form Glen Research (Sterling, VA). This chemically synthesized RNA consists of 28 residues missing the last 5 nucleotides at the 5′-end. Final purity was > 97% as assessed by high pressure liquid chromatography.

Buffer—Protein-RNA interactions were routinely analyzed at 25 °C in a buffer containing 50 mM Tris-HCl, pH 8.0, 50 mM KCl, 1 mM DTT, and 10 mM $MgCl_2$ (standard buffer). Additionally, some of the experiments were also performed in a buffer containing 200 mM KOAc, 50 mM Tris-HCl, pH 7.7, and 10 mM DTT (6). EPR measurements were performed in a buffer containing 50 mM Tris-HCl, pH 7.0, 12 mM NaCl, and 5% glycerol.

Polymerase Activity Determination—RNA-dependent DNA polymerase activity on poly(rA)/oligo$(dT)_{12–18}$ substrates was measured by a standard assay described previously (33, 34) with 2.8 nM RT for 10 min

[2] O. Kensch, unpublished data.

at 37 °C in a buffer containing 50 mM Tris-HCl, pH 8.0, 80 mM KCl, 5 mM DTT, 6 mM $MgCl_2$ and 0.05% (v/v) Triton X-100.

Filter Binding Assay—Protein and 5′-^{32}P-labeled RNA were mixed in standard buffer and incubated at 25 °C for 10 min. An aliquot of this mixture was filtered under suction through a prewet (standard buffer) nitro-cellulose filter (Schleicher & Schuell BA85) and rinsed with 4 ml of standard buffer. Radioactivity retained on the filters was measured by scintillation counting.

Fluorescence Equilibrium Measurements of RT-RNA Binding—The affinity of the different RTs for the pseudoknot RNA was measured both by displacing a fluorescently labeled 18/36-mer DNA/DNA p/t bound to RT and by titrating increasing amounts of RT with 5′-HEX-labeled RNA.

The fluorescently labeled DNA-primer was synthesized by coupling the phosphoroamidite dye 6-carboxyfluorescein, a fluorescein derivative, directly to the 5′-end of the oligodeoxynucleotide during DNA synthesis according to the recommendation of the manufacturer (Applied Biosystems). The titrations were performed using an SLM AB2 spectrofluorometer. To monitor the fluorescence change upon displacing the labeled p/t from RT, the samples were excited at 492 nm, and the emission intensity was measured at 516 nm. These competitive titrations were evaluated using the program Scientist (MicroMath), which allows the user to define the system under investigation as a series of parallel equations defining (in this case) each discrete equilibrium, the relationship between the total and free concentrations of the components, and the way in which the observable signal is generated. The K_d of the 18/36-mer DNA/DNA p/t was determined independently (30, 35) and kept constant during the fit procedure (primer sequence, 5′-TCCCTGTTCGGGCGCCAC-3′; template sequence, 5′-TGTGGAAAATCTCATGCAGTGGCGCCCGAACAGGGA-3′).

To monitor the fluorescence change upon binding of RT to the 5′-HEX-labeled pseudoknot RNA, the samples were excited at 538 nm, and the emission intensity was measured at 556 nm. Data were fitted to a quadratic equation analogous to the one given by Müller *et al.* (36) using the program Grafit (Erithacus Software). Values for the dissociation constant (K_d), the amplitude of the fluorescence change, and the RNA concentration were allowed to vary during the fit procedure.

Rapid Kinetics of RT-RNA Interaction—Experiments on the kinetics of the association of HIV-1 RT with the pseudoknot RNA were performed using a stopped flow apparatus (High Tech Scientific, Salisbury, United Kingdom). 25 nM $Alexa_{488}$-labeled HIV-1 RT (final concentration) was rapidly mixed with increasing 5′-HEX-labeled pseudoknot RNA concentrations (50–300 nM). Collection and analysis of the data was done as described previously (27, 30). Excitation of the $Alexa_{488}$-labeled protein was at 435 nm and detection of the donor quenching due to fluorescence resonance energy transfer to the HEX-fluorophor was through a bandpass filter (520 nm). Data were fitted using a double exponential equation. The rate of the first phase (k_{+1}) is dependent on the concentration of RT and corresponds to the formation of the collision complex. The rate of the second phase (k_{+2}) is largely concentration-independent and arises from a conformational change of the RT-RNA complex after formation of the collision complex.

EPR Measurements—Continuous wave EPR experiments were performed using home made X-band EPR spectrometers equipped with a dielectric resonator (Bruker) or with an H_{103} cavity (AEG). The magnetic field was measured with a B-NM 12 B-field meter (Bruker). Spin-labeled RT samples were loaded into EPR quartz capillaries (50 μl for low temperature measurements, otherwise 5 μl) at a final RT concentration of 100–200 μM. Spectra were recorded with a modulation amplitude of 1.5 G, and the microwave power was adjusted to between 0.2 and 0.6 mW. A modified Oxford ESR 9 variable temperature accessory allowed stabilization of the sample temperature between 80 and 330 K. The whole apparatus was controlled by a personal computer, which also performed 12 bit analog-to-digital data acquisition. EPR powder spectra simulations were performed according to the method described by Steinhoff *et al.* (37).

The spin-spin interaction between two spin labels attached to a protein is composed of static dipolar interaction, modulation of the dipolar interaction by the residual motion of the spin label side chains, and exchange interaction. For temperatures below 200 K, the residual motion of the nitroxide side chain is strongly restricted, and the static dipolar interaction leads to considerable broadening of the spectrum if the interspin distance does not exceed 25 Å. A detailed line shape analysis allows determination of absolute values of the interspin distance in the range of about 10 to 25 Å (37–40). For certain cases the modulation of the dipolar interaction due to the motion of the spin labels allows an estimation of the interresidue distances at room temperature (41). Exchange interaction was found to contribute significantly to the line broadening for distances of less than 10 Å, because partial overlap of the nitrogen pi-orbitals of the two interacting nitroxides is required (42, 43).

RESULTS

Affinity of HIV-1 RT for the Pseudoknot RNA by Equilibrium Binding—Binding measurements to determine the K_d of the RT-RNA complex were performed using three different approaches. Fig. 2*A* shows a displacement titration using a fluorescently labeled DNA/DNA p/t, for which the affinity has previously been determined (35). When this p/t binds to RT, its fluorescence is quenched. A complex was formed between RT and the p/t, and increasing amounts of pseudoknot RNA were added. The fluorescence increase observed upon displacement of the fluorescent p/t into solution was measured, as shown in Fig. 2*A*. A K_d of 25 pM was calculated from a least squares fit of the data to a model describing both equilibria (see under "Experimental Procedures").

Fig. 2*B* shows titration of increasing amounts of HIV-1 RT with a 5′-HEX-labeled pseudoknot RNA. Data were fitted to a quadratic equation yielding a K_d of 24 pM. These results indicate that the chemically synthesized RNA, labeled with a fluorophor on the 5′-end (see under "Experimental Procedures"), shows a similar affinity for RT to the *in vitro* transcribed RNA used in Fig. 2*A*.

However, in Fig. 2, *A* and *B,* the concentration of the substrates is 2–3 orders of magnitude higher than the determined K_d value, and therefore the K_d values derived show a rather large error, being in the same range as the fitted value. Due to the limiting fluorescence signal of the probes, it was not possible to reduce the substrate concentrations below 1 nM. To overcome the drawbacks of fluorescence-based measurements, radioactive labeling was used, allowing for the use of substrate concentrations in the pM range. Fig. 2*C* shows a filter binding assay in which 5′-^{32}P-labeled pseudoknot RNA was titrated with increasing amounts of RT. However, upon dilution of the RNA from the stock solution (which had a concentration in the micromolar range) to the working solution in the low picomolar range, about 90% of the RNA was lost, probably due to molecules irreversibly absorbing to the Eppendorf tube. Several attempts to minimize this problem were only partially successful. However, as the RNA is highly labeled, it was possible to correct for these losses. Fitting of the experimental data, shown in Fig. 2*C,* to a quadratic equation yielded a K_d of about 40 pM, in good agreement with the fluorescence-based approaches. However, this K_d is dependent on the assumption that dilute solutions of RT do not result in absorption to the Eppendorf tube, as seen with the RNA. If such absorption (which cannot easily be corrected for) takes place, the effective protein concentration would be reduced, leading to a lower K_d value than determined. Therefore the figure of 40 pM should be regarded as an upper estimate.

Measurements were performed routinely in standard buffer (50 mM Tris-HCl, pH 8, 50 mM KCl, 1 mM DTT, and 10 mM $MgCl_2$) with refolded pseudoknot RNA. Performing the experiments in the buffer used to select the pseudoknot (50 mM Tris-HCl, pH 7.7, 200 mM KOAc, and 10 mM DTT) and carry out previous experiments (6), with RNA that was not folded, gave similar results.

Kinetics of RT-RNA Association—Stopped flow experiments were performed to analyze the association of RT with RNA. Binding of RT to the 5′-HEX-labeled pseudoknot RNA results in quenching of the fluorescence signal of about 6% (see Fig. 2*B*). This rather small signal change was, however, not sufficient to obtain reasonable data in stopped flow experiments. We therefore used fluorescence resonance energy transfer to enhance the signal. The $Alexa_{488}$-fluorophor (absorption and

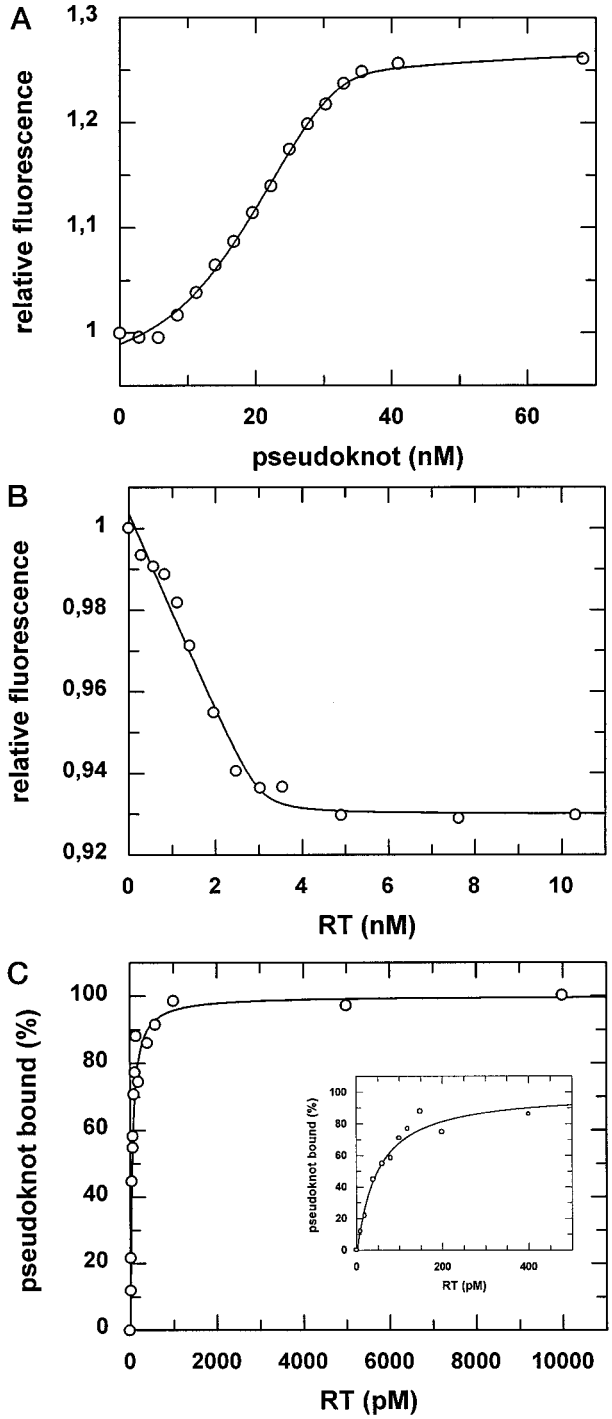

FIG. 2. **Equilibrium titrations of HIV-1 RT and pseudoknot RNA.** *A,* displacement titration of fluorescent p/t bound to HIV-1 RT with pseudoknot RNA. A complex of carboxyfluorescein-labeled 18/36-mer DNA/DNA (25 nM) and RT (40 nM) was titrated with increasing amounts of competitor. The *curve* shows the best fit by least-square fitting to the model describing the two binding equilibria from which a dissociation constant of 25 ± 17 pM for the pseudoknot was obtained (see under "Experimental Procedures"). The sequence of the DNA/DNA p/t is given under "Experimental Procedures." *B,* titration of 5′-HEX-labeled pseudoknot RNA (3 nM) with increasing amounts of HIV-1 RT. The *curve* shows the best fit to a quadratic equation describing the binding of the RNA to a single site in the heterodimeric enzyme. The fit gives a value of 24 ± 39 pM for the K_d. *C,* filter binding assay of radiolabeled RNA with RT. 8 pM 5′-^{32}P-labeled pseudoknot RNA was titrated with increasing amounts of RT. The *curve* shows the best fit to a quadratic equation yielding a K_d of 40 ± 6 pM.

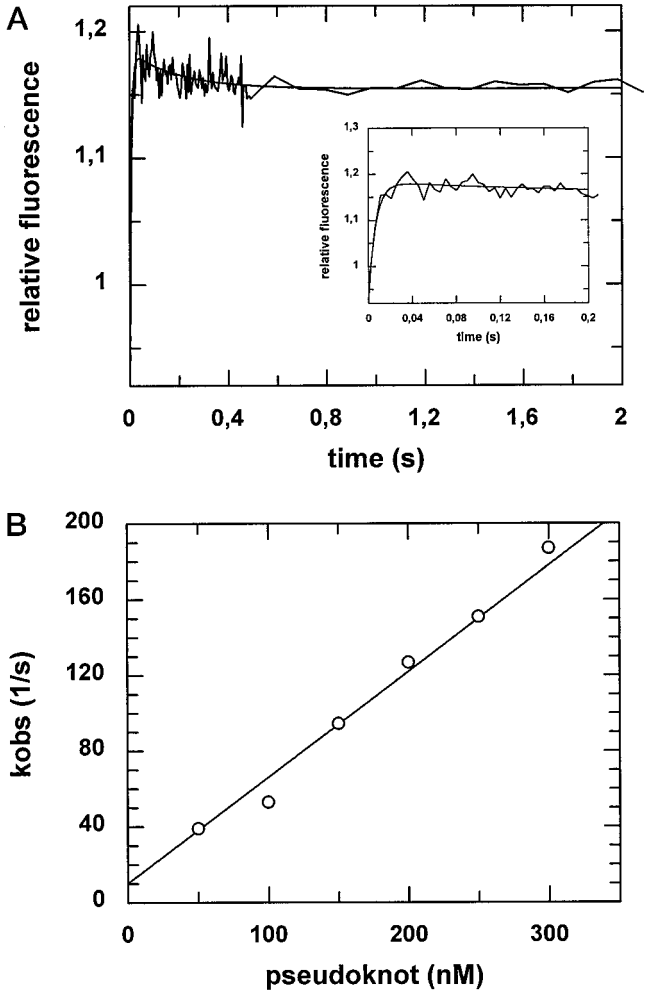

FIG. 3. **Kinetics of the binding of 5′-HEX-labeled pseudoknot RNA to a Alexa$_{488}$-labeled HIV-1 RT (amino acid 281 in p51).** *A,* a typical stopped flow result is shown. A 25 nM sample of RT was rapidly mixed with 250 nM RNA. Excitation was at 435 nm, and the donor emission was detected via a bandpass filter (520 nm). Fitting of the experimental data to a double exponential equation gave rates of 151 ± 6 and 4.9 ± 0.4 s^{-1}. *B,* dependence of the pseudo-first-order rate constant of pseudoknot binding on the RNA concentration. A constant concentration of fluorescently labeled RT (25 nM) was mixed with increasing amounts of 5′-HEX-labeled pseudoknot. k_{+1} and k_{-1} were determined by the slope of the linear fit and the intercept of the line with the *y* axis and yielded values of 5.6 ± 0.4 × 10^8 M^{-1} s^{-1} and 10 ± 8 s^{-1}, respectively.

emission maxima of 493 and 520 nm, respectively) covalently linked to a cysteine at position 281 in the small subunit of the heterodimeric enzyme was used as donor and the HEX-fluorophor (absorption and emission maxima of 538 and 555 nm, respectively) on the 5′-end of the RNA as acceptor. From the x-ray structure of the protein-RNA complex, it could be predicted that the two fluorophors are about 20 Å apart (see Fig. 1). Upon binding of the RNA to the protein, a quenching of the donor fluorescence of about 20% could be observed. Independent measurements demonstrated that the Alexa$_{488}$-labeled enzyme had comparable behavior to wild type RT with respect to enzymatic activities, substrate binding, and affinity for the pseudoknot (data not shown).

Fig. 3*A* shows a typical stopped flow experiment. The data obtained could be fitted best to an equation with two exponential terms. The fast first phase was dependent on the RT concentration, whereas the slower phase was not. In Fig. 3*B,* the dependence of the first phase of pseudoknot binding (observed pseudo-first-order rate constant) on RT concentration is

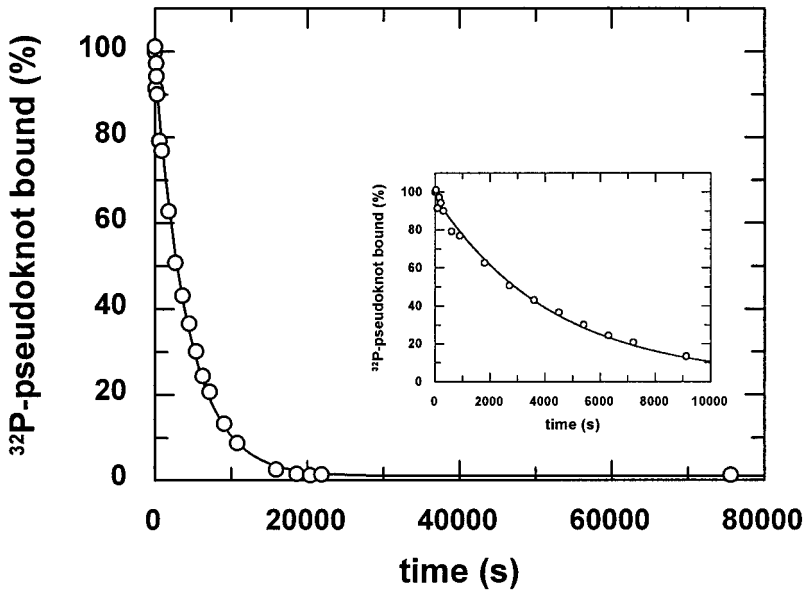

FIG. 4. **Analysis of the dissociation of the protein-RNA complex using a filter binding assay.** 25 nM HIV-1 RT was preincubated with 20 nM 5′-^{32}P-labeled pseudoknot RNA and then mixed with 2 μM unlabeled pseudoknot RNA. Aliquots were analyzed at different time points by spotting onto a nitro-cellulose filter, rinsing with 4 ml of binding buffer, and scintillation counting. The *curve* shows the best fit to a single exponential equation yielding a off-rate of 0.0002 s^{-1}.

shown. The rate constants k_{+1} and k_{-1} are given by the slope of the line and the intercept with the *y* axis, respectively (44). For the first step in pseudoknot binding values for k_{+1} and k_{-1} of 5.6×10^8 M^{-1} s^{-1} and 10 s^{-1} were obtained, in the same range as those observed previously for DNA/DNA and DNA/RNA binding (45).

Analysis of the RT-RNA Dissociation—Attempts to measure the dissociation rate of the protein-RNA complex using stopped flow did not result in an appreciable signal change over the maximal useful time range of the instrument, indicating that this process might be too slow to be measured by this approach. Thus, the filter binding assay was applied to determine the dissociation rate of the complex. 25 nM RT was complexed with 20 nM ^{32}P-labeled RNA and then mixed with 2 μM of unlabeled pseudoknot. Analyses of the amount of radioactive pseudoknot that remained bound at different times (Fig. 4) gave data that fitted to a single exponential, yielding an observed dissociation rate of 0.0002 s^{-1}. Essentially the same rate constant was determined using the 5′-HEX-labeled pseudoknot in a fluorescence spectrofluorometer (data not shown).

Binding of RT to the Pseudoknot RNA by Kinetic Measurements—The results outlined above show that the binding of the pseudoknot RNA to HIV-1 RT can be best described as a two-step process. Scheme 1 summarizes the results obtained form the different kinetic experiments. RT and pseudoknot RNA initially form a collision complex with a second order rate constant of 5×10^8 M^{-1} s^{-1} followed by a slower, concentration-independent isomerization with a rate constant of about 5 s^{-1}. The rate constants determined for the reverse reaction are 0.0002 and 10 s^{-1}. The latter was indirectly derived from the *y* axis intercept of a linear fit of RNA concentration *versus* observed pseudo-first-order rate and therefore is subject to a rather large error (see Fig. 3*B*). Efforts to observe k_{-1} directly by performing double mixing stopped flow experiments did not yield interpretable data (data not shown). A K_d of about 0.8 pM can be calculated from these rate constants, about 30 times lower than determined using equilibrium measurements.

Affinity of HIV-2 and EIAV RT for the Pseudoknot—To investigate the specificity of the interaction of the pseudoknot with HIV-1, RT binding studies were carried out with the closely related RTs of HIV-2 and EIAV. Fig. 5 shows the effect of adding increasing amounts of these RTs to the 5′-HEX-labeled pseudoknot. Fitting the experimental data to a quadratic equation yielded K_d values of 85 and 118 nM for the HIV-2

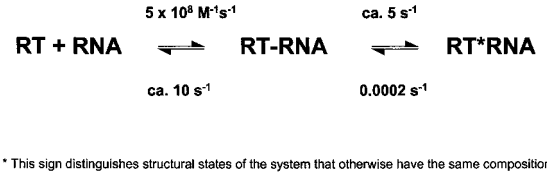

SCHEME 1

and EIAV complexes, respectively. Interestingly, the signal change upon binding of these RTs to the fluorescently labeled RNA is much larger than for HIV-1 RT. In both cases, the fluorescence signal was quenched by about 50%, compared with about 6% in the case of HIV-1 RT. To ensure that the fluorophor is not interfering with binding to the HIV-2 and EIAV RT, we analyzed the interaction by performing displacement titrations using a fluorescently labeled DNA/DNA p/t as described above. These experiments gave essentially the same K_d values (data not shown).

Effect of the RNA on Polymerase Activity of Different RTs—To further illustrate the exceptional specificity of the pseudoknot RNA for the HIV-1 enzyme we performed standard RT assays using poly(rA)/oligo(dT) as substrate. The reactions were started with preincubated RT-RNA complexes. Fig. 6 shows the effect of the pseudoknot RNA on the polymerase activity of HIV-1, HIV-2 and EIAV RT. At pseudoknot concentrations at which the HIV-1 enzyme is fully inhibited with respect to the polymerase activity, there is only a minor effect on HIV-2 and EIAV RT, as would be predicted from the different K_d values evaluated above. The difference in the observed K_i values (defined as the pseudoknot concentration that inhibited polymerase activity by 50%) is given by a factor of about 3.5×10^4.

EPR Measurements—Site-directed spin labeling has emerged as a powerful technique for exploring the structure and dynamics of both soluble and membrane proteins (for a recent review, see Ref. 46). We have applied this method to determine in solution the relative positions of the fingers and thumb domains of the p66 subunit of RT, both as an unliganded apo-enzyme and in the presence of bound nucleic acids, and have compared these data with data obtained from x-ray analysis (for a review, see Ref. 1). RT was mutagenized to introduce two unique cysteines in the p66 subunit. Subsequent reaction with a thiol specific nitroxide resulted in an RT variant carry-

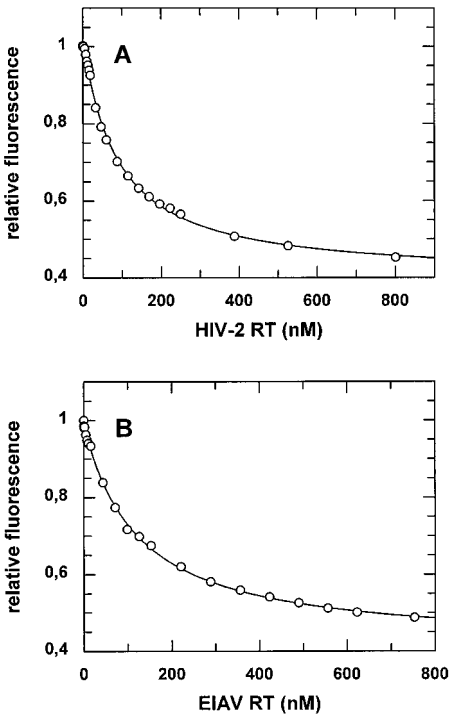

FIG. 5. **Binding of the pseudoknot RNA to HIV-2 and EIAV RT.** 5′-HEX-labeled pseudoknot RNA (7 nM) was titrated with increasing amounts of HIV-2 (*A*) and EIAV (*B*) RT. The curves show the best fit to a quadratic equation yielding K_d values of 85 ± 4 and 118 ± 4 nM for the HIV-2 and EIAV enzymes, respectively.

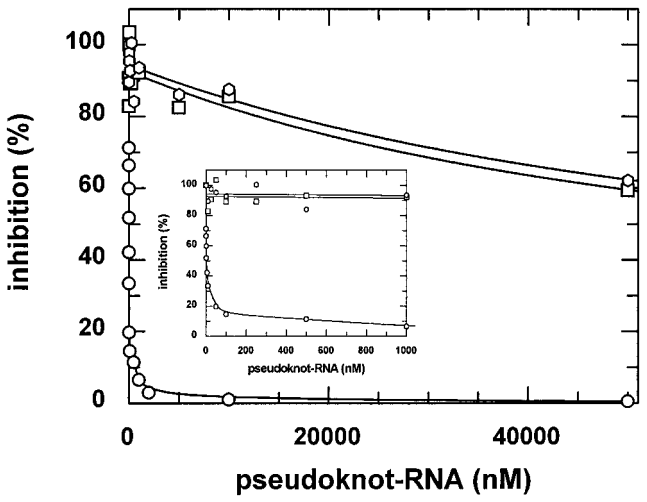

FIG. 6. **Standard RT assay with different RTs in the presence of pseudoknot RNA.** RNA-dependent DNA polymerase activity on poly(rA)/oligo(dT)$_{12-18}$ substrates (approximately 1.2 μM with respect to the free 3′-ends) was measured for 10 min at 37 °C. 2.8 nM HIV-1 (*circles*), HIV-2 (*squares*), and EIAV (*hexagons*) RT were preincubated with increasing amounts of pseudoknot RNA. The reaction was initiated by the addition of the RT-RNA complexes to the assay mixture.

ing two spin labels, one at the tip of the fingers and the second in the thumb domain (amino acids 24 and 287, respectively; see Fig. 1). EPR spectroscopy was used to determine the distance between these spin labels.

The EPR spectra of spin-labeled RT liganded to either a DNA/DNA p/t (18/36-mer) or the pseudoknot RNA were measured at 170 K in frozen solution to exclude dynamic effects and motional averaging of the dipolar broadening. Room temperature measurements (293 K) were performed to characterize the mobility of the spin label side chains and to study spin-spin interaction at a more physiological temperature. The EPR spectra were normalized to represent the same number of spins. The results, shown in Fig. 7, reveal considerable line broadening for the RT bound to RNA compared with the enzyme bound to DNA. Powder spectra simulations were performed to determine absolute values for the interspin distances (37). The experimental spectra are generally composed of species with different relative nitroxide orientations and interspin distances because of the flexibility of the spin label side chains and the variety of conformational substates of the proteins in frozen solution. A fitting of simulated EPR spectra to the experimental data with the assumption of a Gaussian interspin distance distribution yields an average interspin distance, d, and the distance distribution width, σ, which also accounts for small amounts of singly spin-labeled proteins. The parameters that describe the EPR spectrum in the absence of any spin-spin interaction were fixed according to the values obtained from the fitting of simulated powder spectra to the experimental data of spin-labeled proteins in a similar environment (47). The respective values are given in the legend to Fig. 7. The experimental and simulated spectra with interspin distances >21 Å for the DNA-bound species and 13 Å for the RNA-bound structure agree well (Fig. 7).

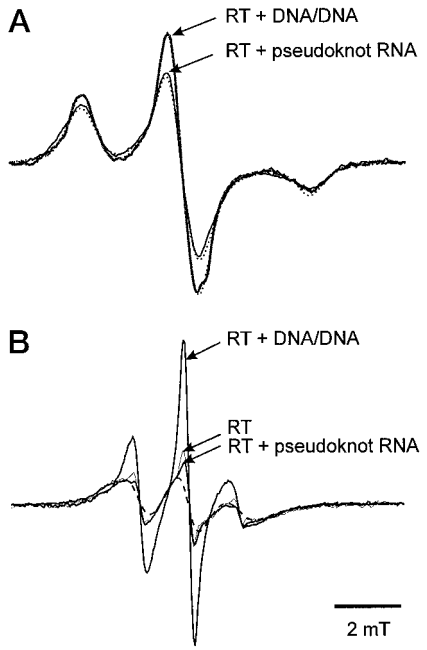

FIG. 7. **EPR spectra of the spin-labeled RT double mutant p66^{W24C_R1,K287C_R1} (R1 = (1-oxyl-2,2,5,5-tetramethylpyrroline-3-methyl)methane-thiosulfonate; see under "Experimental Procedures").** *A,* spectra of RT + DNA/DNA (*thick trace*) and RT + pseudoknot RNA were recorded at 170 K and normalized to constant spin number. The *dotted traces* show fits of dipolar broadened powder spectra with interspin distances of >21 Å (RT + DNA/DNA) and 13Å (RT + pseudoknot RNA). Parameters taken from spectra of noninteracting spin labels and kept fixed during the fitting procedure were as follows: g_{xx} = 2.0089, g_{yy} = 2.0065, g_{zz} = 2.0026, A_{xx} = 5.4 G, A_{yy} = 4.9 G, A_{zz} = 36.5 G, and a field-independent line shape function composed of a superposition of 53% Lorentzian and 47% Gaussian of 4.8 and 4.1 G width, respectively. *B.* room temperature spectra of the RT double mutant with bound DNA/DNA or pseudoknot RNA (*heavy traces*) and without substrate (*light trace*) normalized to constant spin number. The *dashed trace* shows the convolution of the of the spectrum of the DNA/DNA-bound RT with a Lorentzian broadening function of line width, ΔDH = 6 G, which gives the best fit to the dipolar broadened spectral fraction of the pseudoknot RNA-bound RT.

At room temperature, the spin label side chain motion occurs in the nanosecond time range, and the nitroxide mobility and the flexibility of the protein backbone are directly reflected in the EPR absorption line shape. The small apparent hyperfine splitting visible in the spectrum of the DNA-bound RT indi-

cates high mobility of the nitroxide side chains. This spectral shape is typical for nitroxide side chains bound to flexible loop regions as revealed by the comparison with spectra of 1-oxyl-2,2,5,5-tetramethylpyrroline-3-methyl)methane-thiosulfonate bound to the E-F cytoplasmic loop of bacteriorhodopsin (48). The lack of any additional spectral component of considerable amplitude reveals that the dynamics of both nitroxide side chains must be very similar. In the RNA-bound species of RT, the apparent hyperfine splitting is only slightly increased, indicating only minor changes in the tertiary interaction of the nitroxides compared with the DNA-bound structure. However, the line width is substantially increased, which must be due to spin-spin interaction. The spectrum of the RNA-bound RT can be fit reasonably well by the convolution of a Lorentzian function with the spectrum of the DNA-bound species. The nonbroadened contribution to the spectrum is most probably due to a small fraction of singly labeled species, which amounts to less than 10%. The broadening appears to be homogeneous across the spectrum, and the line width at half height, ΔDH, of the Lorentzian provides a quantitative measure of the spin-spin interaction (41). The best fit is obtained with $\Delta DH = 6$ G, which yields an interspin distance of 12.5 Å according to the empirical calibration given by Mchaourab *et al.* (41). Due to the high flexibility of the nitroxides and because we do not distinguish between exchange and dipolar interaction, this value has to be regarded as an estimate of the average interspin distance. Additionally, as the line width depends on r^{-6}, the average is weighted in favor of molecules with smaller interspin distances. With this in mind, the estimated distance value agrees well with that determined from the low temperature experiment.

At room temperature, the spectrum of the substrate free RT is nearly indistinguishable from that of the RNA-bound species. Because the spectral shape of this mutant is determined by the spin-spin interaction, this result is strong evidence that the finger-thumb distance of the main fraction of the free RT is identical to that of the RNA-bound structure.

DISCUSSION

Comparing the x-ray structure of the pseudoknot RNA-RT complex (20) with that of RT bound to a DNA/DNA p/t (49, 50), reveals that the RNA makes more extensive contacts with the enzyme than the natural substrate does. The DNA duplex contacts mainly the p66 subunit of the RT heterodimer, showing interactions close to the polymerase active site (fingers and thumb domain) and the RNaseH active site. The inhibitory RNA also shows interactions with these regions of the enzyme. Additionally, there are extensive interactions with the small (p51) subunit. The RNA, therefore, sits snugly in the nucleic acid binding cleft, in contrast to DNA/DNA duplexes, which appear to "float" above this cleft. For the complex of RT with a DNA duplex, a K_d of about 2 nM has previously been determined (35). On the basis of the available structural information, which indicates less extensive interactions of DNA/DNA as compared with the RNA inhibitor, we performed a detailed biochemical examination of the RT-pseudoknot RNA interaction. In particular, we suspected that the binding might be considerably stronger than what has been published by others (6).

Equilibrium binding experiments using fluorescently as well as radioactively labeled RNA yielded K_d values of about 25 pM for the enzyme inhibitor complex. As described above (see under "Results"), binding studies in the low picomolar range are technically problematic due to experimental limitations that are difficult to overcome. We therefore regard the value of 25 pM as an upper limit, meaning that the interaction could be even tighter. Interestingly, we observed similar binding affinities regardless of the salt concentration of the buffer (50–200 mM). Additionally, refolding of the RNA in a buffer containing $MgCl_2$ using a standard protocol was not necessary to obtain tight binding. The only difference seen was in the time required for the fluorescence signal to become stable in titration experiments when the RNA was not refolded, indicating that the proper folding might be induced and stabilized upon interacting of the pseudoknot with RT. However, it is not know whether Mg^{2+} is important for the folding of this RNA in the absence of the enzyme.

The kinetic analysis of the RT-pseudoknot interaction revealed that binding occurs in two steps, previously shown for DNA/DNA or DNA/RNA binding to the enzyme (45). The observed on-rates for complex formation are in the same range as for the nucleic acid duplex substrates, whereas the off-rates are much slower explaining the extraordinarily tight binding. Calculating the K_d of the complex using the kinetic constants given in Scheme 1 gives a value of 0.8 pM, about 30 times lower than what has been determined via the equilibrium binding experiments. This obvious discrepancy could be explained by either the k_{-1} value not being entirely correct, because it was determined indirectly, by the determined equilibrium K_d being too high for technical reasons, as described above, or by a combination of both. Nevertheless, the two K_d values are in reasonable agreement when the limitations of the techniques used are considered.

An important aspect concerning the pseudoknot RNA aptamer is the specificity of the interaction with HIV-1 RT. This is interesting not only in terms of the selectivity index of this inhibitor but also with respect to the potential of the SELEX method to select for highly specific ligands. Binding studies with HIV-2 and EIAV RTs yielded K_d values of 85 and 118 nM, respectively. This dramatic reduction in affinity in comparison to HIV-1 RT was an especially surprising finding because the HIV-2 RT used in this study shows 60% identity and 13% homology to the HIV-1 enzyme. On the basis of this result, we propose that in addition to the overall fold of the pseudoknot, there must be site-specific interactions between protein and RNA that are responsible for the tight binding to HIV-1 RT, because it is likely that the HIV-2 enzyme adopts a comparable structure and therefore should be capable of forming similar overall interactions. This could be an explanation for the sequence conservation seen in stem 1 among the minimal Tuerk-type pseudoknots (8). Unfortunately, the resolution of the x-ray structure of the RT-RNA complex (about 4.8 Å) is not sufficient to clearly identify such interactions.

The conformation of RT observed in the x-ray structure of the RNA complex resembles the closed conformation, in which fingers and thumb of p66 are in close contact, also seen in the structure of the unliganded enzyme (21, 51). This conformation is stabilized by the RNA through extensive electrostatic interactions with several basic residues in helix I of the p66 thumb and in the p66 fingers domain. From the crystal structure described by Rodgers *et al.* (21), it cannot be deduced whether RT adopts this closed conformation in solution because it cannot be ruled out that this structure is induced and/or stabilized by crystal packing. Consequently, there is no clear answer to the question of whether the pseudoknot RNA was selected against the closed conformation of RT, as recently proposed (20), or alternatively whether the protein-RNA interaction has induced a closure of the thumb domain relative to the fingers domain. To address these questions, we performed EPR measurements, analyzing the interspin distances of spin labels attached to the tip of the fingers and thumb domain in p66. The solution structure at 293 K of RT complexed with the RNA pseudoknot shows a distance of 13 Å between the spin labels at

positions Cys-24 and Cys-287 in the large subunit. This value is in excellent agreement with the distance of 12 Å between Cβ from Trp-24 and Lys-287 found in the crystal structure of the RT-pseudoknot complex (20). Furthermore, the EPR spectra of unliganded and pseudoknot-complexed RT are virtually indistinguishable, clearly showing for the first time that RT adopts the closed conformation in solution at room temperature. Thus, the pseudoknot RNA appears to have been selected against this structure, indicating that neither the RNA nor the protein undergoes significant conformational change upon complex formation, which would further account for the extraordinarily low K_d for this interaction.

Typically, RNA aptamers selected for tight binding to protein targets show binding constants in the low nanomolar to micromolar range (52). Occasionally tighter binding, with K_d values of 100–500 pM, is reported. However, to our knowledge, an RNA aptamer with a binding constant of $\leq$25 pM has not been described so far. This aptamer shows binding at least 100-fold tighter than that of the natural substrate, exceptional specificity, and a broad working range concerning buffer conditions, making it an encouraging drug candidate for the treatment of HIV infections. Experiments are in progress to evaluate the inhibitory potential of this pseudoknot RNA in cell tissue culture.

Acknowledgments—We thank Karin Vogel-Bachmayr and Martina Wischnewski for excellent technical assistance, Manfred Souquet for purifying the EIAV RT, Paul Rothwell for purifying the $Alexa_{488}$-labeled HIV-1 RT, Joachim Jäger for providing Fig. 1, and Jochen Reinstein and Birgitta Wöhrl for fruitful discussions.

REFERENCES

1. Jäger, J., and Pata, J. D. (1999) *Curr. Opin. Struct. Biol.* **9,** 21–28
2. De-Clercq, E. (1999) *I/Farmaco* **54,** 26–45
3. Vandamme, A. M., Van Laethem, K., and De-Clercq, E. (1999) *Drugs* **57,** 337–361
4. Gold, L. (1995) *J. Biol. Chem.* **270,** 13581–13584
5. Tuerk, C., and Gold, L. (1990) *Science* **249,** 505–510
6. Tuerk, C., Macdougal, S., and Gold, L. (1992) *Proc. Natl. Acad. Sci. U. S. A.* **89,** 6988–6992
7. Green, L., Waugh, S., Binkley, J. P., Hostomska, Z., Hostomsky, Z., and Tuerk, C. (1995) *J. Mol. Biol.* **247,** 60–68
8. Burke, D. H., Scates, L., Andrews, K., and Gold, L. (1996) *J. Mol. Biol.* **264,** 650–666
9. Rietveld, K., Van Poelgeest, R., Pleij, C. W., Van Boom, J. H., and Bosch, L. (1982) *Nucleic Acids Res.* **10,** 1929–1946
10. Studnicka, G. M., Rahn, G. M., Cummings, I. W., and Salser, W. A. (1978) *Nucleic Acids Res.* **5,** 3365–3387
11. Ferre-D'Amare, A. R., Zhou, K. H., and Doudna, J. A. (1998) *Nature* **395,** 567–574
12. Deiman, B. A. L. M., and Pleij, C. W. A. (1997) *Semin. Virol.* **8,** 166–175
13. Puglisi, J. D., Wyatt, J. R., and Tinoco, I. J. (1990) *J. Mol. Biol.* **214,** 437–453
14. Shen, L. X., and Tinoco, I. (1995) *J. Mol. Biol.* **247,** 963–978
15. Du, Z. H., Giedroc, D. P., and Hoffman, D. W. (1996) *Biochemistry* **35,** 4187–4198
16. Du, Z. H., Holland, J. A., Hansen, M. R., Giedroc, D. P., and Hoffman, D. W. (1997) *J. Mol. Biol.* **270,** 464–470
17. Kang, H. S., and Tinoco, I. (1997) *Nucleic Acids Res.* **25,** 1943–1949
18. Kolk, M. H., Vandergraaf, M., Wijmenga, S. S., Pleij, C. W. A., Heus, H. A., and Hilbers, C. W. (1998) *Science* **280,** 434–438
19. Su, L., Chen, L. Q., Egli, M., Berger, J. M., and Rich, A. (1999) *Nat. Struct. Biol.* **6,** 285–292
20. Jäger, J., Restle, T., and Steitz, T. A. (1998) *EMBO J.* **17,** 4535–4542
21. Rodgers, D. W., Gamblin, S. J., Harris, B. A., Ray, S., Culp, J. S., Hellmig, B., Woolf, D. J., Debouck, C., and Harrison, S. C. (1995) *Proc. Natl. Acad. Sci. U. S. A.* **92,** 1222–1226
22. Ho, S. N., Hunt, H. D., Horton, R. M., Pullen, J. K., and Pease, L. R. (1989) *Gene* **77,** 51–59
23. Müller, B., Restle, T., Weiss, S., Gautel, M., Sczakiel, G., and Goody, R. S. (1989) *J. Biol. Chem.* **264,** 13975–13978
24. Le Grice, S. F., Naas, T., Wohlgensinger, B., and Schatz, O. (1991) *EMBO J.* **10,** 3905–3911
25. Certa, U., Bannwarth, W., Stüber, D., Gentz, R., Lanzer, M., Legrice, S. F. J., Gulliot, F., Wendler, I., Hunsmann, G., Bujard, H., and Mous, J. (1986) *EMBO J.* **5,** 3051–3056
26. Müller, B., Restle, T., Kühnel, H., and Goody, R. S. (1991) *J. Biol. Chem.* **266,** 14709–14713
27. Souquet, M., Restle, T., Krebs, R., Legrice, S. F. J., Goody, R. S., and Wöhrl, B. M. (1998) *Biochemistry* **37,** 12144–12152
28. Wöhrl, B. M., Krebs, R., Thrall, S. H., Le Grice, S. F. J., Scheidig, A. J., and Goody, R. S. (1997) *J. Biol. Chem.* **272,** 17581–17587
29. Thrall, S. H., Krebs, R., Wöhrl, B. W., Cellai, L., Goody, R. S., and Restle, T. (1998) *Biochemistry* **37,** 13349–13358
30. Krebs, R., Immendorfer, U., Thrall, S. H., Wöhrl, B. M., and Goody, R. S. (1997) *Biochemistry* **36,** 10292–10300
31. Sambrook, J., Fritsch, E. F., and Maniatis, T. (1994) *Molecular Cloning: A Laboratory Manual*, Cold Spring Harbor Laboratory, Cold Spring Harbor, NY
32. McGregor, A., Murray, J. B., Adams, C. J., Stockley, P. C., and Connolly, B. A. (1999) *J. Biol. Chem.* **274,** 2255–2262
33. Restle, T., Müller, B., and Goody, R. S. (1990) *J. Biol. Chem.* **265,** 8986–8988
34. Jacques, P. S., Wöhrl, B. M., Ottmann, M., Darlix, J. L., and Le Grice, S. F. J. (1994) *J. Biol. Chem.* **269,** 26472–26478
35. Divita, G., Müller, B., Immendörfer, U., Gautel, M., Rittinger, K., Restle, T., and Goody, R. S. (1993) *Biochemistry* **32,** 7966–7971
36. Müller, B., Restle, T., Reinstein, J., and Goody, R. S. (1991) *Biochemistry* **30,** 3709–3715
37. Steinhoff, H. J., Radzwill, N., Thevis, W., Lenz, V., Brandenburg, D., Antson, A., Dodson, G., and Wollmer, A. (1997) *Biophys. J.* **73,** 3287–3298
38. Steinhoff, H. J., Dombrowsky, O., Karim, C., and Schneiderhahn, C. (1991) *Eur. Biophys. J.* **20,** 293–303
39. Rabenstein, M. D., and Shin, Y. K. (1995) *Proc. Natl. Acad. Sci. U. S. A.* **92,** 8239–8243
40. Thorgeirsson, T. E., Xiao, W. Z., Brown, L. S., Needleman, R., Lanyi, J. K., and Shin, Y. K. (1997) *J. Mol. Biol.* **273,** 951–957
41. Mchaourab, H. S., Oh, K. J., Fang, C. J., and Hubbell, W. L. (1997) *Biochemistry* **36,** 307–316
42. Closs, G. L., Forbes, M. D. E., and Piotrowiak, P. (1992) *J. Am. Chem. Soc.* **114,** 3285–3294
43. Fiori, W. R., and Millhauser, G. L. (1995) *Biopolymers* **37,** 243–250
44. Rittinger, K., Divita, G., and Goody, R. S. (1995) *Proc. Natl. Acad. Sci. U. S. A.* **92,** 8046–8049
45. Wöhrl, B. M., Krebs, R., Goody, R. S., and Restle, T. (1999) *J. Mol. Biol.* **292,** 333–344
46. Hubbell, W. L., Gross, A., Langen, R., and Lietzow, M. A. (1998) *Curr. Opin. Struct. Biol.* **8,** 649–656
47. Tiebel, B., Radzwill, N., Aung-Hilbrich, L. M., Helbl, V., Steinhoff, H. J., and Hillen, W. (1999) *J. Mol. Biol.* **290,** 229–240
48. Pfeiffer, M., Rink, T., Gerwert, K., Oesterhelt, D., and Steinhoff, H. J. (1999) *J. Mol. Biol.* **287,** 163–171
49. Jacobo-Molina, A., Ding, J., Nanni, R. G., Clark, A. D., Lu, X., Tantillo, C., Williams, R. L., Kamer, G., Ferris, A. L., Clark, P., Hizi, A., Hughes, S. H., and Arnold, E. (1993) *Proc. Natl. Acad. Sci. U. S. A.* **90,** 6320–6324
50. Huang, H., Chopra, R., Verdine, G. L., and Harrison, S. C. (1998) *Science* **282,** 1669–1675
51. Hsiou, Y., Ding, J., Das, K., Clark, A. D., Jr., Hughes, S. H., and Arnold, E. (1996) *Structure* **4,** 853–860
52. Patel, D. J., Suri, A. K., Jiang, F., Jiang, L., Kumar, P. F., and Nonin, S. (1997) *J. Mol. Biol.* **272,** 645–664